EARTHQUAKE ENGINEERING AND STRUCTURAL DYNAMICS
Earthquake Engng Struct. Dyn. 2013; **00**:1–14
Published online in Wiley InterScience (www.interscience.wiley.com). DOI: 10.1002/eqe

Adaptive multi-rate interface: development and experimental verification for real-time hybrid simulation

Amin Maghareh [1,*,†], Jacob P. Waldbjoern [2], Shirley J. Dyke [1,3], Arun Prakash [1], and Ali I. Ozdagli [1]

[1] *Lyles School of Civil Engineering, Purdue University, West Lafayette, USA*
[2] *Department of Civil Engineering, Technical University of Denmark, Copenhagen, Denmark*
[3] *School of Mechanical Engineering, Purdue University, West Lafayette, USA*

SUMMARY

Real-time hybrid simulation (RTHS) is a powerful cyber-physical technique which provides a framework for global/local system evaluation of civil structures subject to extreme dynamic loading. Due to the need for meeting hard real-time constraints, one of the major factors which determines the ability of the RTHS to represent the true system level behavior is the numerical substructure. Higher-order finite element models entail additional demand for computational resources, which in turn may limit achievable sampling frequencies and/or introduce delays that can degrade stability and performance in RTHS. The goal of this research is to develop a new multi-rate compensation interface to effectively enable the use of more complex numerical models, running at a slower sampling rate, coupled with an experimental substructure, running at a higher sampling rate. The effectiveness of the proposed method is experimentally verified. Furthermore, a set of simulated studies are implemented to systematically compare the performance of the proposed method to existing methods. Compared to existing methods, the proposed technique incorporates a built-in delay compensation feature, leads to smaller error, especially, at higher sampling frequency ratios and input signals with high-frequency content, and does not induce spurious oscillations at the coupling frequency.

Received . . .

KEY WORDS: Real-time hybrid simulation; RTHS; Multi-rate RTHS; mrRTHS

1. INTRODUCTION

As civil engineering structures evolve to meet the needs of future generations, there is an increasing demand to address ongoing challenges such as demonstrating the effectiveness of performance-based design, considering soil-structure interaction, and utilizing new materials capable of reducing earthquake impact [6]. These challenges justify the need for extending and evolving our experimental capabilities for evaluating structural response and performance in a suitable and cost-effective manner. The necessity to assess the dynamic performance of rate-dependent structural components, and recent advances in systems with hard real-time computing capabilities, have led researchers to conduct real-time hybrid simulation (RTHS). With the introduction of new seismic mitigation techniques and devices, such as rubber bearings, viscous dampers, friction dampers, sloshing dampers, magneto-rheological dampers and electro-rheological dampers, earthquake engineers have developed new techniques to evaluate structural dynamic performance using hybrid

*Correspondence to: Amin Maghareh, Intelligent Infrastructure Structure Systems Laboratory, Purdue University, West Lafayette, IN, USA.
†Email address: amaghare@purdue.edu

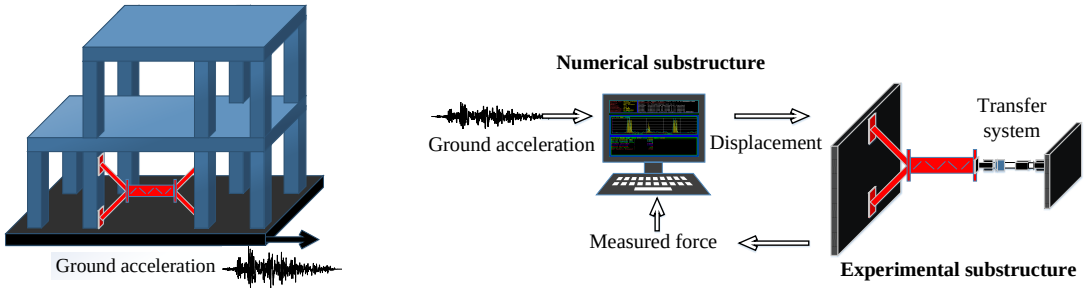

(a) Reference structure (b) Real-time hybrid simulation

Figure 1. A typical real-time hybrid simulation of a civil structure.

simulation, which imposes hard real-time constraints on the digital components. In RTHS, the interface interaction between the substructures is enforced by servo-hydraulic actuators or a shake table which acts as the transfer system. This transfer system must be controlled to ensure that all interface boundary conditions are satisfied in real time. Figure 1 depicts a real-time hybrid simulation of a two-story structure where hydraulic actuators are used to satisfy the interface boundary conditions.

The power of hybrid simulation (HS) and real-time hybrid simulation lies in its promise to accelerate the rate at which research in earthquake engineering is conducted. In the past decade, an increasing number of researchers have utilized HS methods as an alternative to quasi-static or shake table testing. The capability of HS and RTHS to capture both, the local response of individual structural components and the global system behavior, under realistic loading allows great flexibility. Unlike shake-table tests that are constrained by size and shape of the structure, HS and RTHS can be conducted on different types of structures in different loading configurations [5]. Many projects have used HS/RTHS to investigate a variety of topics related to seismic and wind engineering. Recently, researchers have begun to rely on HS or RTHS to assess local and global responses, to compare various aspects related to design guidelines, particularly design codes [9].

In classical RTHS, global stability and performance dictate the sampling frequency [14], and it is usually chosen to be an integer multiple of the digital servo-controller's sampling frequency, such as 1024Hz [3]. Due to stringent real time constraints and the fact that the time required to solve a high-order numerical model is usually much greater than the RTHS time-step, low-order numerical models that usually do not require a significant amount of time to solve are chosen by researchers, see Figure 2. These simplified low-order models are limited in their ability to represent the underlying dynamics of the numerical substructure, especially for complex and/or non-linear systems. To overcome this challenge, two approaches are available: parallel real-time computing and multi-rate RTHS (mrRTHS).

Parallel real-time computing has the potential to enable execution of computationally intensive numerical models in RTHS. However, currently there are very few openly available platforms that are suitable for writing and executing parallel computations in real time [7]. Most current real-time systems only support sequential processing, in which a real-time workload may use only one processor core at a time, or multi-processing, in which a real-time workload may use multiple independent processor cores. Recently, a computational platform based on a federated scheduling model that exploits both intra-task and inter-task parallelism, was developed to enable execution of high fidelity numerical models within the real-time constraints of RTHS [8].

In multi-rate RTHS, the numerical substructure (or a portion of it) is executed at a slower rate than the experimental substructure. Running the numerical substructure at a slower rate provides more time to complete the task of time integration for more complex finite element (FE) models, see Figure 3. However, in order to implement mrRTHS successfully from stability and performance perspectives, an effective rate-transitioning method is needed to compute the command signal properly. In this study, we propose a new rate-transitioning scheme, posted in the George E. Brown

DOI: 10.1002/eqe

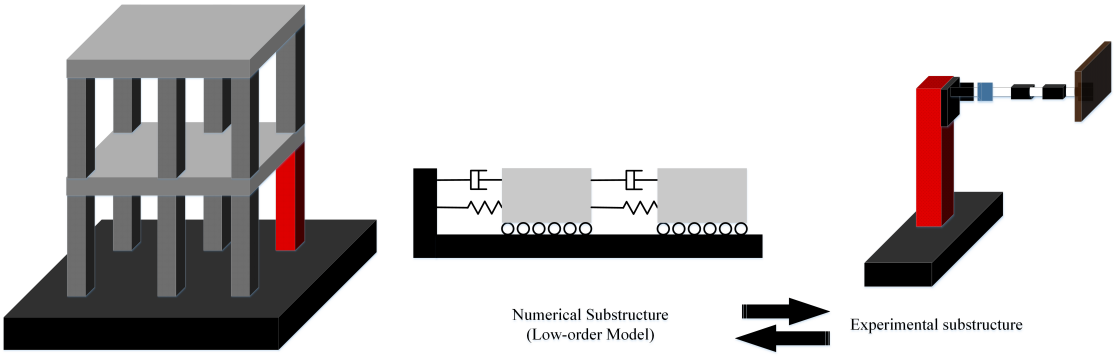

(a) Reference structure (b) Real-time hybrid simulation

Figure 2. Conventional RTHS with computationally-inexpensive numerical substructure.

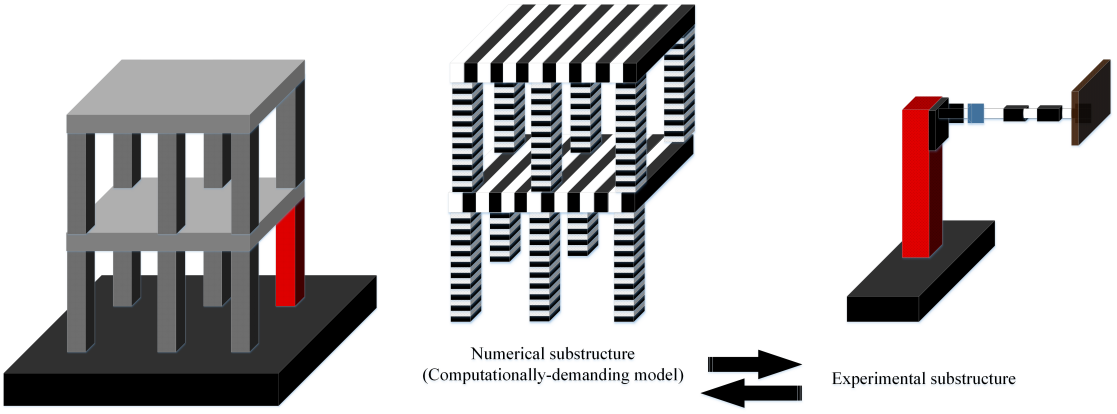

(a) Reference structure (b) Real-time hybrid simulation

Figure 3. RTHS with computationally-expensive numerical substructure.

Network for Earthquake Engineering Simulation (http://www.nees.org/resources/tools). Also, a new evaluation procedure for the use of rate-transitioning techniques in mrRTHS is proposed and compared to some of the existing techniques.

The concept of multi-rate RTHS was first developed by Nakshima and Masaoka due to the computing/processing limitations in the late 90's [15]. In their RTHS setup, a novel sub-stepping technique was developed so that the experimental substructure is continuously loaded. Their computer executes two tasks: (1) the task of creating the target displacement by solving the equations of motion with an integration time interval of Δt, called Response Analysis Task, and (2) the task of creating successive displacement signals with a smaller time interval of δt (to ensure smooth actuator motion) and sending the signals to the digital servo-controller, called Signal Generation Task. The computation of the numerical substructure was executed at each main integration time step, Δt, while a smooth command signal generation task is also executed at each sub-step, δt. The two tasks are computationally independent and separated. The sub-stepping technique, combined with the use of priority based multi-tasking, produced a smooth command signal for the experimental substructure [16, 15]. This work was later pursued by Bonnet [1] who introduced a new multi-tasking strategy.

In this paper, we develop new rate-transitioning and compensation techniques that enable researchers to simulate the numerical substructure (or a part of it) at a slower execution rate than the experimental substructure. This approach facilitates the use of complex, high-fidelity numerical models and thus reduces modeling error in RTHS. To evaluate the performance of

DOI: 10.1002/eqe

different rate-transitioning techniques, a metric is developed, and the performance of the proposed technique is compared with three existing rate-transitioning techniques in a set of multi-rate numerical simulations. Finally, the newly-developed rate-transitioning and compensation technique is experimentally validated for multi-degree-of-freedom mrRTHS.

2. RATE-TRANSITIONING TECHNIQUES

Currently, three methods are available that allow the numerical and experimental substructures to run at two different rates in an RTHS. When multi-rate approaches are used, the numerical substructure is integrated using a coarse integration time. Between two consecutive data points from the numerical substructure, a finer control signal is generated through a rate-transitioning scheme. The first two methods are based on polynomial extrapolation and the third method is based on linearly predicted acceleration. Herein, we define some recurring symbols in this section:
Δt: coarse integration incerement
δt: fine integrarion incerement
SFR: sampling frequency ratio ($\Delta t/\delta t$)

2.1. Existing methods

Method I: This method was developed by Bonnet, see [1]. In this method, the control signal is extrapolated through a compensation method developed by Horiuchi *et al.* in [12, 10] using current and previous data points from the numerical substructure. For an N^{th} order polynomial fit, a number of $N+1$ data points are needed in the following equation:

$$d_{exp} = \sum_{i=0}^{N} a_i d_i \tag{1}$$

where d_{exp}, d_i, and a_i are the control signal with a time step of δt, the current and previous displacements with a time step of Δt, and polynomial coefficients generated through the Lagrange polynomials, respectively. The original prediction scheme in [12] assumes identical time step for d_{exp} and d_i. For that reason, Bonnet reformulated a more general expression for a_i allowing a fully independent time step for d_{exp} and d_i using a third order polynomial fitting scheme.

$$a_1 = \frac{\delta t}{\Delta t}[\frac{11}{6} + \frac{\delta t}{\Delta t} + \frac{1}{6}(\frac{\delta t}{\Delta t})^2] \tag{2a}$$
$$a_2 = -\frac{\delta t}{\Delta t}[\frac{3}{1} + \frac{5}{2}\frac{\delta t}{\Delta t} + \frac{1}{2}(\frac{\delta t}{\Delta t})^2] \tag{2b}$$
$$a_3 = \frac{\delta t}{\Delta t}[\frac{3}{2} + 2\frac{\delta t}{\Delta t} + \frac{1}{2}(\frac{\delta t}{\Delta t})^2] \tag{2c}$$
$$a_4 = -\frac{\delta t}{\Delta t}[\frac{1}{3} + \frac{1}{2}\frac{\delta t}{\Delta t} + \frac{1}{6}(\frac{\delta t}{\Delta t})^2] \tag{2d}$$

Method II: The second polynomial method was established by Wallace *et al.* using least-square polynomial fitting, see [18]. As in Method I, the command signal is extrapolated using the current and previous data points computed in the numerical substructure. A polynomial of order N with coefficients a_i ($i \in \{0, \cdots, N\}$) is fit using least-squares.

$$y = a_0 + a_1 x + \cdots + a_N x^N \tag{3}$$

Given N data points $\{(x_0, y_0) \cdots (x_{N-1}, y_{N-1})\}$, the polynomial coefficients can be computed using the following equation:

$$\begin{pmatrix} 1 & 0 & \cdots & 0 \\ 1 & -\Delta t & \cdots & \Delta t^{N-1} \\ \vdots & \vdots & \ddots & \vdots \\ 1 & -(N-1)\Delta t & \cdots & [-(N-1)\Delta t]^{N-1} \end{pmatrix} \begin{pmatrix} a_0 \\ a_1 \\ \vdots \\ a_N \end{pmatrix} = \begin{pmatrix} y_0 \\ y_1 \\ \vdots \\ y_{N-1} \end{pmatrix} \tag{4}$$

DOI: 10.1002/eqe

and, X_p is the forward prediction vector given by:

$$X_p = [1\ p\Delta t\ \cdots\ p^N \Delta t^N] \tag{5}$$

where p is the number of time steps to be predicted and the predicted point d_{exp} is computed as:

$$d_{exp} = X_p[a_0 \cdots a_N]^T. \tag{6}$$

Method III: A third method by Horiuchi and Konno is based on the assumption that there is a linear acceleration as a function of time, see [11]. The extrapolated command signal for a smaller time step δ_t is given by:

$$d_{exp} = d_0 + \delta t \dot{d}_0 + \frac{1}{3}\delta t^2 \ddot{d}_0 + \frac{1}{6}\delta t^2 \ddot{d}_{exp} \tag{7}$$

where $\ddot{d}_{exp}$ is the predicted acceleration after δt given by:

$$\ddot{d}_{exp} = 2\ddot{d}_0 - \ddot{d}_1. \tag{8}$$

This calculation requires the current velocity and acceleration. However, only the velocity and acceleration from the previous time step is available. Thus, Horiuchi and Konno proposed a method to overcome this issue, see [11].

Although these techniques are effective at low sampling frequency ratios (about 1-5), at higher sampling frequency ratios (≥ 5), they may either lead to significant chattering at the coupling frequency or even instabilities. Therefore, a new technique is proposed and shown to be effective at high sampling frequency ratios as well as low sampling frequency ratios. Furthermore, with the proposed technique, no additional time-delay compensation is required.

2.2. Adaptive multi-rate interface

An adaptive multi-rate interface (AMRI) is developed, allowing the numerical and experimental substructures to run at two different rates, enabling the use of computationally-demanding numerical models while maintaining a good actuator tracking control. Here, the numerical substructure is executed with a coarse integration time, referred to as Δt. After selecting a set of bases, such as polynomial or exponential, sampling frequency ratio between the numerical and experimental substructures, and compensation time, a finer control signal is generated using the proposed method with a fine integration time, referred as δt. Herein, we define some of AMRI's parameters:
X: input signal w/ coarse integration increment Δt
Y: output signal w/ fine integration increment δt
SFR: sampling frequency ratio ($\Delta t/\delta t$)
M: number of α coefficients
R: number of orthogonal bases used for interpolation
r: interpolation order
p: compensation coefficient, $p\Delta t$ is time to be compensated.

In AMRI, $N + M + p - 1$ displacement points (current and previous) with the integration increment of Δt are used to generate SFR+1 points of displacement commands with the integration increment of δt. As examples, four cases with 1-step and 3-step compensation and sampling frequency ratios of 5 and 10 are provided in Figure 4.

Figure 5 shows a simplified framework in which adaptive multi-rate linear compensation can be used in the implementation of mrRTHS. For a better understanding of how the proposed rate-transitioning scheme functions, AMRI computations are divided into three sequential steps: compensation, extrapolation, and interpolation.

Compensation: In this step, Equation (9) is used to compensate and predict the command signal,

$$C(z) = \alpha_1 \times z^{-p} + \alpha_2 \times z^{-p-1} + \cdots + \alpha_M \times z^{-p-M+1} \tag{9}$$

DOI: 10.1002/eqe

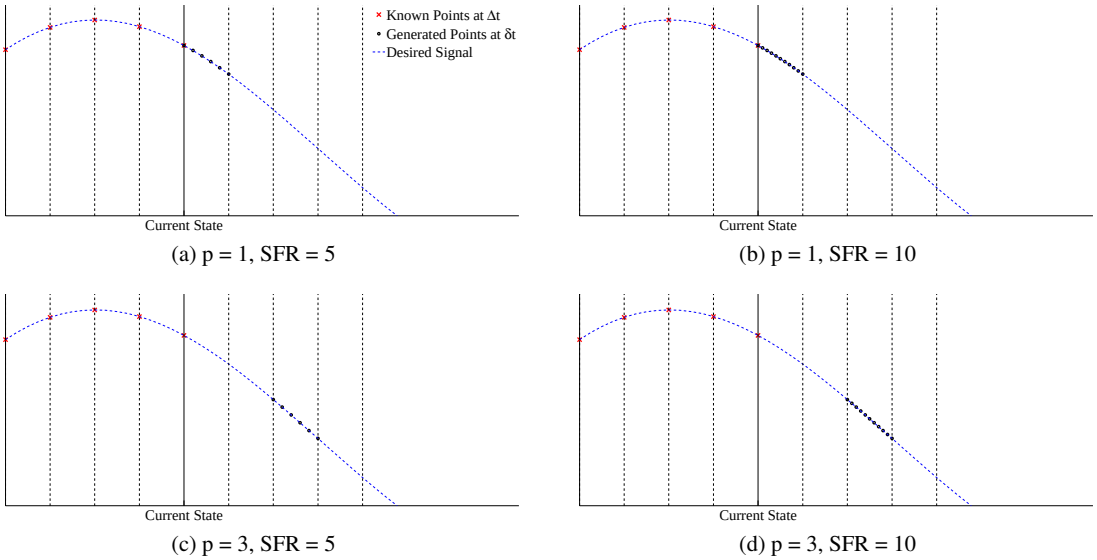

(a) p = 1, SFR = 5 (b) p = 1, SFR = 10

(c) p = 3, SFR = 5 (d) p = 3, SFR = 10

Figure 4. Adaptive multi-rate linear compensation.

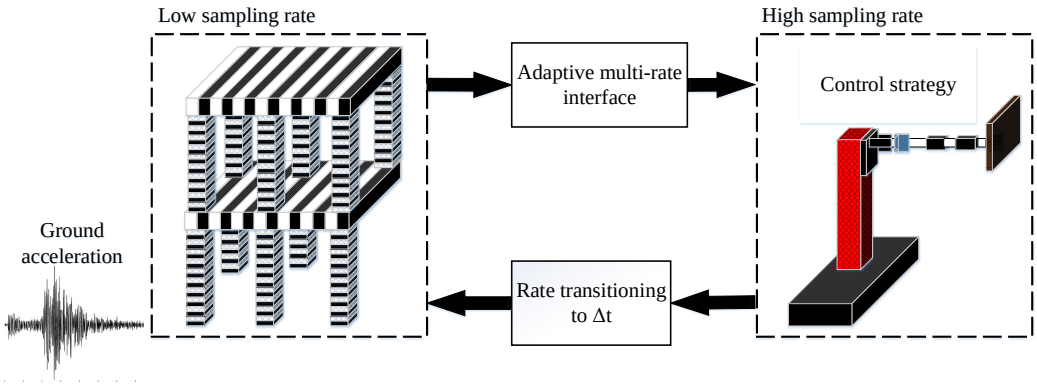

Figure 5. Use of adaptive multi-rate linear compensation in multi-rate RTHS.

where $p\Delta t$ is the compensated time, $p \in \{1, 2, 3 \cdots\}$ and z is the complex variable in the Z-domain. Equation (9) is a time-varying, discrete transfer function and the coefficients $\{\alpha_1, \alpha_2 \cdots \alpha_M\}$ are obtained at each time step by solving the following least-squares equation:

$$\begin{pmatrix} X_{n-p-N+1} & X_{n-p-N} & \cdots & X_{n-p-N-M+2} \\ \vdots & \vdots & \ddots & \vdots \\ X_{n-p} & X_{n-p-1} & \cdots & X_{n-p-M+1} \end{pmatrix}_{N\times M} \times \begin{pmatrix} \alpha_1 \\ \alpha_2 \\ \vdots \\ \alpha_M \end{pmatrix} = \begin{pmatrix} X_{n-N+1} \\ X_{n-N+2} \\ \vdots \\ X_n \end{pmatrix}. \qquad (10)$$

DOI: 10.1002/eqe

Extrapolation: After obtaining the α values, the next p points $\{X_{n+1}, \cdots, X_{n+p}\}$ are extrapolated using Equation 11.

$$\begin{pmatrix} X_{n-p+1} & X_{n-p} & \cdots & X_{n-p-M+2} \\ \vdots & \vdots & \ddots & \vdots \\ X_n & X_{n-1} & \cdots & X_{n-M+1} \end{pmatrix}_{p\times M} \times \begin{pmatrix} \alpha_1 \\ \alpha_2 \\ \vdots \\ \alpha_M \end{pmatrix} = \begin{pmatrix} X_{n+1} \\ X_{n+2} \\ \vdots \\ X_{n+p} \end{pmatrix} \tag{11}$$

Interpolation: In this step, Chebyshev polynomials of the first kind are used as a set of orthonormal bases for interpolation and rate transitioning from Δt to δt. The Chebyshev polynomials of the first kind are defined by the following recurrence relation:

$$T_1(s) = 1, T_2(s) = s, \cdots, T_{n+1}(s) = 2sT_n(s) - T_{n-1}(s) \tag{12}$$

These polynomials must be adjusted to be within a general range of $[a, b]$, where, $a = (p + r - 1)\Delta t$ and $b = p\Delta t$. For this adjustment, $s = \frac{2x-(a+b)}{b-a}$ where x corresponds to a variable in the range [-1, 1]. The first five polynomials are shown in Figure 6. Next, the following linear equation is solved to obtain $\{\beta_1, \beta_2 \cdots \beta_R\}$:

$$\begin{pmatrix} T_1[(p+1-r)\Delta t] & \cdots & T_R[(p+1-r)\Delta t] \\ \vdots & \ddots & \vdots \\ T_1[(p)\Delta t] & \cdots & T_R[(p)\Delta t] \end{pmatrix}_{r\times R} \times \begin{pmatrix} \beta_1 \\ \beta_2 \\ \vdots \\ \beta_R \end{pmatrix} = \begin{pmatrix} X_{n-r+p+1} \\ \vdots \\ X_n \\ \vdots \\ X_{n+p} \end{pmatrix} \tag{13}$$

using the β coefficients, the command signal at the higher sampling time δt can be computed as follows:

$$Y(h) = \beta_1 T_1(h) + \beta_2 T_2(h) + \cdots + \beta_R T_R(h) \tag{14}$$

where $h \in \{(n + p - 1)\Delta t, (n + p - 1)\Delta t + \delta t, (n + p - 1)\Delta t + 2\delta t \cdots (n + p)\Delta t\}$.

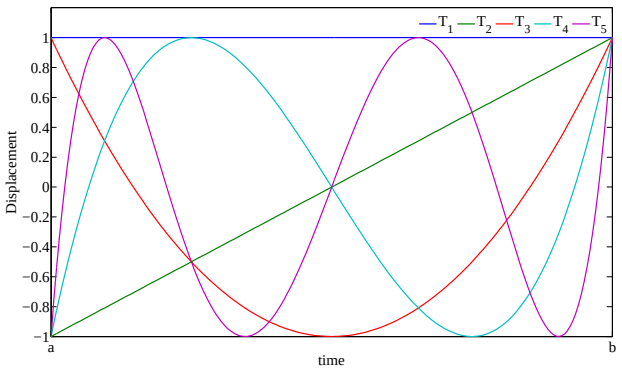

Figure 6. First 5 adjusted Chebyshev polynomials for the general range [a, b].

Tuning factor: In addition, a tuning factor is defined to enable the researcher to effectively set the compensation time while tuning the transfer system. The tuning factor can be monitored in real time or used as a post-experiment tracking performance assessment measure. It is based on a dimensionless index which is computed as follows:

$$TF_i = \frac{norm_2([x^d_{i+n-p-N-M+2} \cdots x^d_{i+n-p}] - [x^m_{i+n-N-M+2} \cdots x^m_{i+n}])}{norm_2([x^m_{i+n-N-M+2} \cdots x^m_{i+n}])} \tag{15}$$

DOI: 10.1002/eqe

where x^d and x^m refer to the desired and measured signals, respectively. The proposed method allows user to set (and tune) the required compensation time ($= p \times \Delta t$). Four different cases are available to assist a user in tuning the compensation constant p, i) increase p by 2, ii) increase p by 1, iii) p value is set, and iv) drop p by 1. The closer set to the reference line, which is the x-axis ($TF = 0$), determines what change, if any, is needed for a better tracking result.

3. VERIFICATION OF ADAPTIVE MULTI-RATE INTERFACE

3.1. Simulated case studies

Tracking performance evaluation of the transfer system is a necessary preliminary step in RTHS. To evaluate the performance of AMRI, three case studies of transfer system tracking dynamics are simulated, see Figure 7. The transfer system model (servo-hydraulic actuator), identified in the

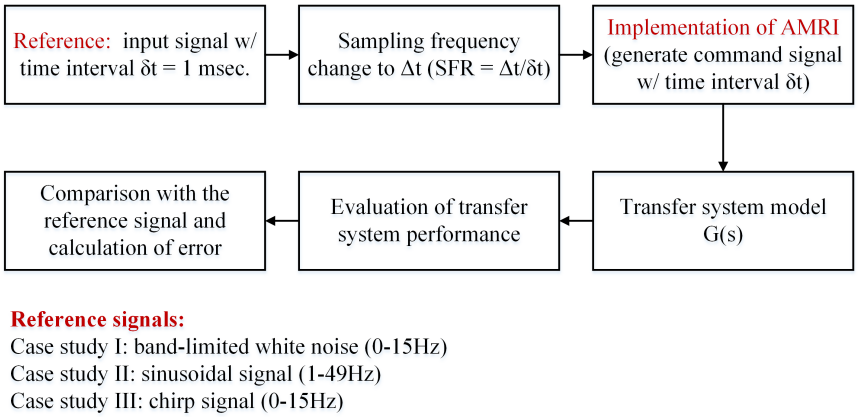

Figure 7. Procedure used to evaluate the AMRI performance for various reference signals (case studies I-III).

Intelligent Infrastructure Systems Lab at Purdue University, is used in this study where transfer function of the plant from command to measured displacement is modeled by:

$$G(s) = \frac{4.52 \times 10^9}{s^4 + 577s^3 + 3.68 \times 10^5 s^2 + 6.28 \times 10^7 s + 4.93 \times 10^9}. \tag{16}$$

Case study I: In this study, the desired signal is band-limited white noise with a cut-off frequency at 15Hz. The sampling frequency ratio is set to be 5, such that the transfer system is running at 1000Hz. It is shown in Figure 8 that the tracking performance using the adaptive multi-rate strategy is smooth and 5 msec delay is well-compensated. The proposed method allows the user to set (and tune) the required compensation time ($= p \times \Delta T$), see Figure 9. The four cases are, i) increase p by 2, ii) increase p by 1, iii) p value is set, and iv) drop p by 1. The closer set to the reference line determines what change is needed for a better tracking result. In addition, in Figure 10, coefficients of the adaptive compensation method are shown. A normalized tracking error is computed as:

$$NE\% = \frac{max(|x^i_{sim} - x^i_{ref}|)}{max(|x^i_{ref}|)} \times 100 \tag{17}$$

and $NE\%$ is smaller than 1%.

Case study II: Two significant strengths of the adaptive multi-rate interface are its effective performance for input signals with high-frequency content and large sampling frequency ratios. To evaluate the performance of the proposed interface, a series of simulated case studies are implemented in which the input is a sinusoidal signal with various frequencies (1-49Hz) and sampling frequency ratios (2, 4, 5, 8, and 10). The corresponding normalized tracking errors using Equation 17 are shown in Figure 11.

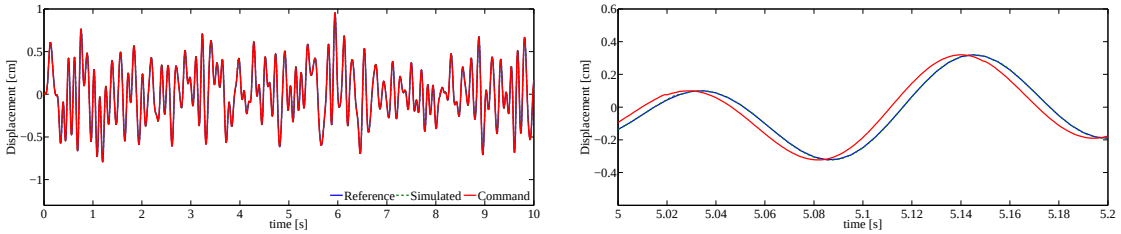

(a) Zoomed-out (b) Zoomed-in

Figure 8. Simulation results of transfer system tracking.

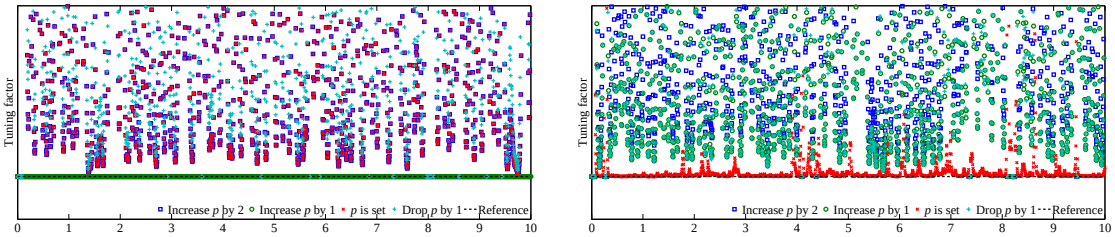

(a) Under-compensated (p needs to increase by 1) (b) Compensation value is well-tuned

Figure 9. Tuning factor and setting p value.

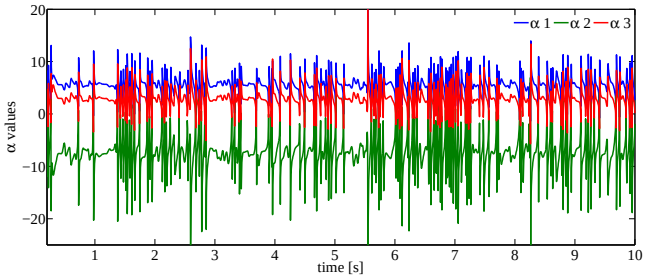

Figure 10. Coefficients of the adaptive compensation method in case study I.

The simulation results shown in Figure 11 allow user to have a better understanding of the error stemming from the multi-rate implementation of a real-time hybrid simulation using AMRI. In this analysis, the frequency spectrum of the command signal is assumed to be known. For instance, the shaded region in Figure 11 results in less than 5% transfer system tracking error AMRI rate-transitioning scheme. Moreover, Figure 11 shows that the majority of cases leads to less than 1% error.

Case study III: Finally, to systematically compare the performance of the three existing methods (method I-III) and AMRI, a set of actuator tracking simulations are conducted with one time step (Δt) compensation and various sampling frequency ratios of 2, 5, 8, and 10. In these simulations, the desired displacement is a chirp signal (0-15Hz). A normalized tracking error is computed as:

$$NRMSE\% = \frac{(\frac{1}{n-1}\sum_{i=1}^{n}(x_{sim}^{i} - x_{ref}^{i})^2)^{1/2}}{max(|x_{ref}^{i}|)} \times 100 \tag{18}$$

where NRMSE stands for normalized root mean square error. The errors are presented in Figure 12 and show that:

- The proposed method exhibits significantly smaller error due to the sampling frequency rate transition for all sampling frequency ratios when compared to Methods I, II, and III.

DOI: 10.1002/eqe

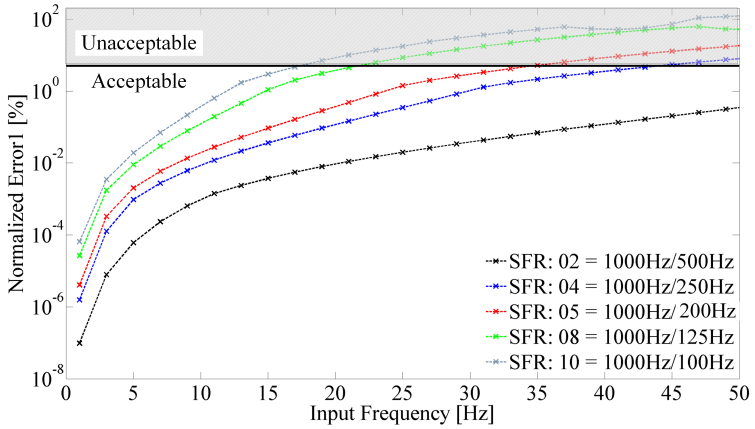

Figure 11. Determining acceptable/unacceptable ranges for a specific multi-rate implementation error.

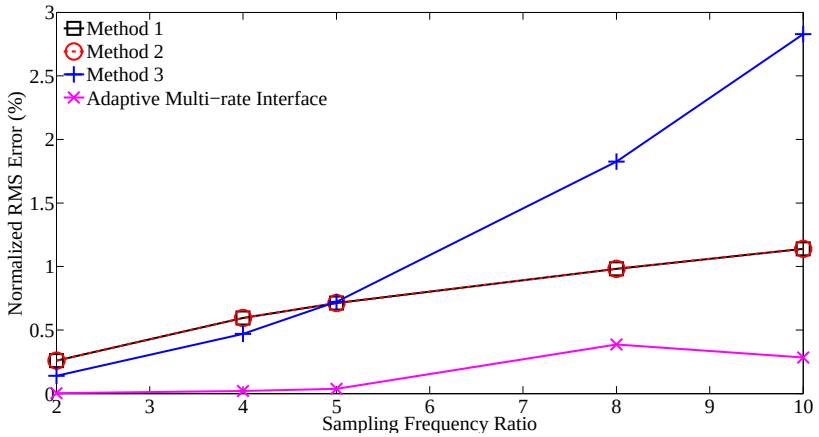

Figure 12. Tracking performance of different rate-transitioning methods.

- Method I and method II exhibit identical performance in the simulated cases.
- Method III performs better than method 1 and 2 for smaller sampling frequency ratios but is not effective for larger sampling frequency ratios.

3.2. RTHS case studies

To evaluate the impact of modeling error and implement the proposed adaptive multi-rate technique, three real-time hybrid simulations are conducted. In these experiments, the numerical substructure is the 9-story structure [17] designed by Brandow and Johnston Associates (1996) for the SAC phase II steel project. The 9-story structure is well-studied as one of the benchmark control structures for seismically-excited nonlinear buildings in [4]. Two models with different levels of refinement are used for the numerical substructure: a 184 degree-of-freedom finite element model constructed using RT-Frame2D open-source software available at [2] and a 9 degree-of-freedom shear model with similar dynamic characteristic at [13]. In this study, the excitation is the N-S component of the El Centro earthquake recorded at the Imperial Valley Irrigation District substation in El Centro, California, during the Imperial Valley, California earthquake of 18 May 1940. The seismic responses and main dynamic characteristics of the two models are provided in Figure 13. Figure 13 shows that the simple 9-story shear building model is able to capture the dominant dynamics of the more refined finite element model.

DOI: 10.1002/eqe

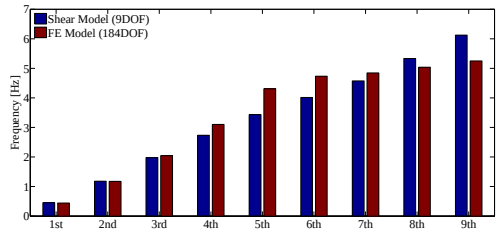

(a) Comparison of modal frequencies.

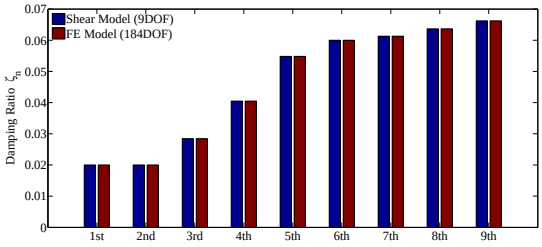

(b) Comparison of modal damping.

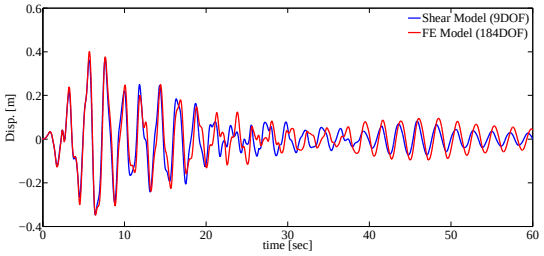

(c) Displacement response.

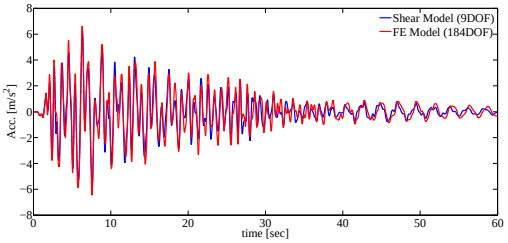

(d) Acceleration response.

Figure 13. Comparison of responses obtained from two numerical models.

Experiment 1 (reference): For the purpose of comparing the performance of the proposed AMRI technique, we designate the response from the real-time hybrid simulation of the 9-story structure where the numerical model is chosen to be the detailed finite element model and run at 1024Hz as the *reference response*. In this RTHS, the experimental substructure is an MR-damper placed on the first floor (between node 9 and node 16), see Figure 14. It should be noted that due to the computational demands of the FE model, the numerical substructure cannot be implemented on an xPC real-time target machine and high-performance xPC (Speedgoat) real-time target system is used instead.

Due to the numerical substructure being computationally demanding, three approaches may be considered: (i) obtaining the best simplified model using model reduction techniques, and using it for RTHS; (ii) using different techniques such as real-time parallel computing to enhance the available computational power; and (iii) using a multi-rate RTHS strategy to run the numerical substructure at a slower rate while the experimental substructure is run at a higher rate. However, currently there are very few openly available platforms that are suitable for writing and executing parallel computations in real-time [19] and [7] and none are yet integrated for RTHS. In this case study, approaches (i) and (iii) are considered and the corresponding responses are compared.

Experiment 2 (RTHS): In the second experiment, a simplified numerical model is adopted and RTHS is conducted at 1024Hz sampling rate on an xPC real-time target machine, see Figure 15.

Experiment 3 (mrRTHS): Finally, a multi-rate RTHS using AMRI with sampling ratio $4 = 1024/256$ was implemented on an xPC real-time target machine, see Figure 16.

Discussions: The results of these experiments are provided in Figure 17. The results show that the proposed technique enables users to implement complicated experiments using a commonly available real-time target system. By comparing the responses, the following observations can be made:

- Modeling idealization error in the numerical substructure can considerably degrade the global RTHS response. As is also evident from Figures 13(c) and (d) the shear model captures the dominant dynamics of the finite element model. However, this insignificant modeling mismatch leads to considerable displacement and acceleration errors in the global response, see Figures 17(a) and (c).

DOI: 10.1002/eqe

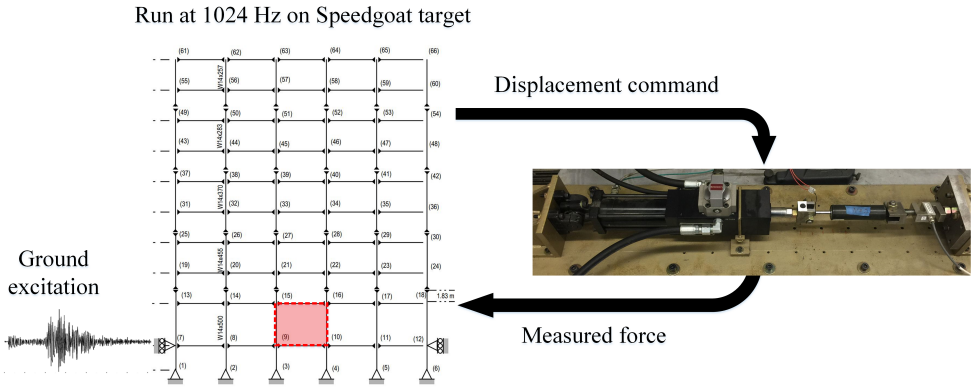

Figure 14. Reference, conventional RTHS with 1024Hz sampling rate and FE numerical substructure.

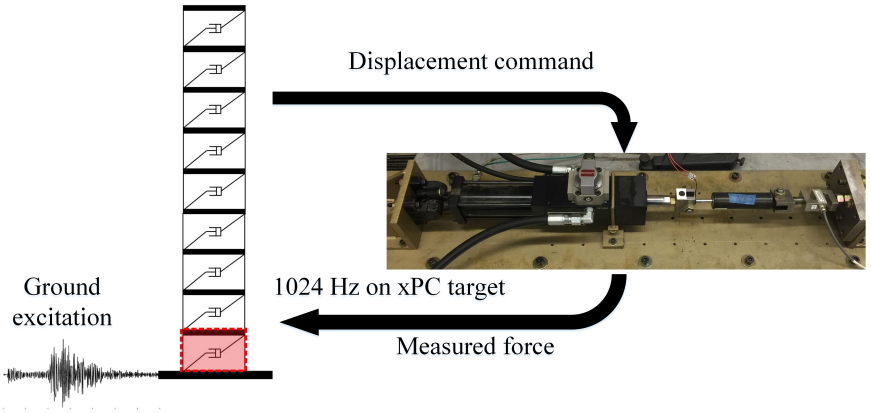

Figure 15. Typical RTHS with 1024Hz sampling rate and shear model numerical substructure.

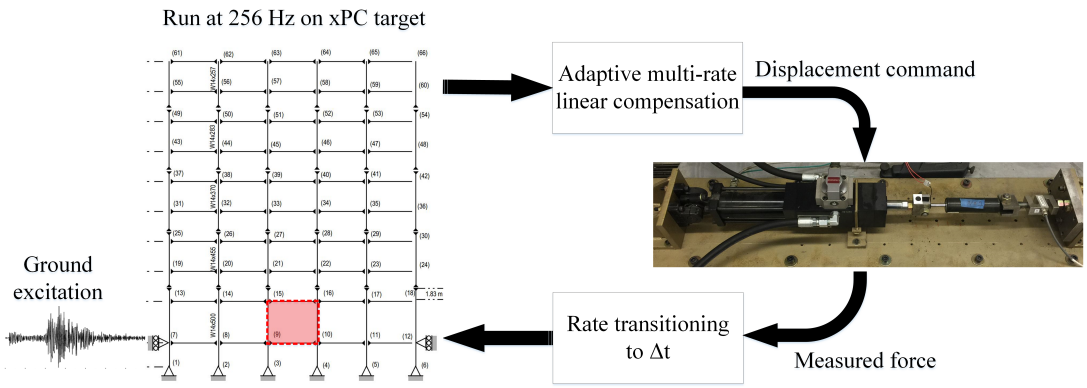

Figure 16. Multi-rate RTHS with sampling ratio 4 (= 1024/256).

- The multi-rate RTHS technique is more effective and leads to a smaller global error than reducing the numerical substructure to a more simplified model, see Figure 16.

4. CONCLUSIONS

One major factor that determines the ability of RTHS to represent realistic behavior of the reference system is the fidelity of the numerical substructure. However, in real-time hybrid simulation, because

DOI: 10.1002/eqe

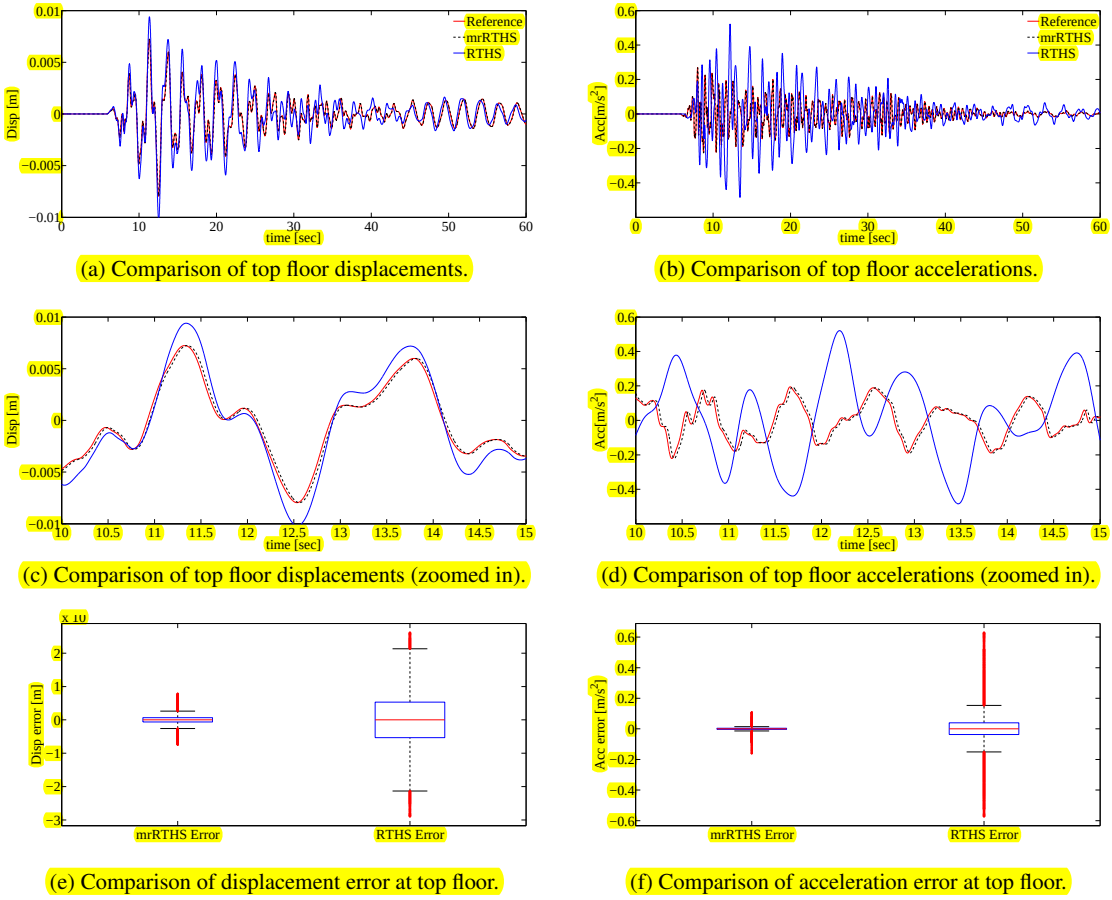

(a) Comparison of top floor displacements.

(b) Comparison of top floor accelerations.

(c) Comparison of top floor displacements (zoomed in).

(d) Comparison of top floor accelerations (zoomed in).

(e) Comparison of displacement error at top floor.

(f) Comparison of acceleration error at top floor.

Figure 17. Comparison of RTHS responses.

of stringent real time constraints, high-fidelity FE models which require a significant time to solve are unsuitable. Thus, researchers established a multi-rate approach in which the computationally-demanding part of the numerical substructure is implemented at a slower rate, while the rest of the structure is executed at a higher rate to achieve a smooth, stable tracking performance. In this study, an adaptive multi-rate interface is developed to effectively enable the use of more complex numerical models, running at a slower sampling rate, coupled with an experimental substructure, running at a higher sampling rate. The effectiveness of AMRI is experimentally verified.

In this experiment, we show that mrRTHS technique is more effective and leads to a smaller global error than reducing the numerical substructure to a more simplified model. Also, we demonstrate that modeling error in the numerical substructure can considerably degrade the global RTHS response. An apparently insignificant modeling mismatch may lead to considerable displacement and acceleration errors in the global response. To mitigate this error, a user can integrate AMRI in RTHS to implement a high-fidelity FE model as numerical substructure. Furthermore, a set of simulated case studies were implemented to systematically compare the performance of the existing methods and the new method. Compared to existing methods, the proposed technique include a built-in delay compensation feature, leads to smaller errors, specifically at higher sampling frequency ratios $\frac{\Delta t}{\delta t}$ and input signals with high-frequency content, and generate smooth and continuous command signal.

DOI: 10.1002/eqe

ACKNOWLEDGEMENT

This material is based upon work supported by the National Science Foundation Graduate Research Fellowship under Grant No. CCF-1136075. The authors would also like to acknowledge the financial support from, the Danish Centre for Composite Structures and Materials (DCCSM) funded by the Danish Council for Strategic Research within Sustainable Energy and Environment (Grant: 09-067212), COWI foundation, and Otto Moensted Foundation.

REFERENCES

1. P. A. Bonnet. The Development of Multi-axis Real-time Substructure Testing. 2006.
2. N. Castaneda-Aguilar, X. Gao, and S. J. Dyke. RT-Frame2D: A Computational Platform for the Real-Time Hybrid Simulation of Dynamically-excited Steel Frame Structures. 2012.
3. C. Chen and J. M. Ricles. Improving the Inverse Compensation Method for Real-time Hybrid Simulation through a Dual Compensation Scheme. *Earthquake Engineering & Structural Dynamics*, 38(10):1237–1255, August 2009.
4. S. J. Dyke, A. K. Agrawal, J. M. Caicedo, R. Christenson, H. Gavin, E. Johnson, S. Nagarajaiah, S. Narasimhan, and B. Spencer. Database for Structural Control and Monitoring Benchmark Problems. 2010.
5. S. J. Dyke, N. Nakata, and G. Marshall. Report on the discussions during the hybrid simulation workshop. 2013.
6. S. J. Dyke, B. Stojadinovic, P. Arduino, M. Garlock, N. Luco, J. A. Ramirez, and S. Yim. 2020 Vision for Earthquake Engineering Research: Report on an OpenSpace Technology Workshop on the Future of Earthquake Engineering. 20(5), 2010.
7. D. Ferry, J. Li, M. Mahadevan, K. Agrawal, C. D. Gill, and C. Lu. A Real-Time Scheduling Service for Parallel Tasks. *IEEE Real-Time and Embedded Technology and Applications Symposium (RTAS'13)*, 2013.
8. D. Ferry, A. Maghareh, G. Bunting, A. Prakash, K. Agrawal, C. Gill, C. Lu, and S. J. Dyke. On the performance of a highly parallelizable concurrency platform for real-time hybrid simulation. *6WCSCM*, 2014.
9. D. Gomez, S. J. Dyke, and A. Maghareh. Enabling role of hybrid simulation within the NEES in advancing earthquake engineering practice and research. 2014.
10. T. Horiuchi, M. Inoue, T. Konno, and W. Yamagishi. Development of a Real-time Hybrid Experimental System Using a Shaking Table (Proposal of Experimental Concept and Feasibility Study with Rigid Secondary System). *JSME International*, 42(2):255–264, 1999.
11. T. Horiuchi and T. Konno. A new method for compensating actuator delay in real-time hybrid experiments. *Philosophical Transactions of the Royal Society A: Mathematical, Physical and Engineering Sciences*, 359:1893–1909, 2001.
12. T. Horiuchi, M. Nakagawa, M. Sugano, and T. Konno. Development of a Real-time Hybrid Experimental System with Actuator Delay Compensation. *Proc. of 11th World Conf. Earthquake Engineering*, 1996.
13. A. Maghareh, M. Barnes, and Z. Sun. Evaluation of the 9-Story Benchmark Building Shear Model, 2012.
14. A. Maghareh, S. J. Dyke, A. Prakash, and J. F. Rhoads. Establishing a Stability Switch Criterion for Effective RTHS Implementation. *Journal of Smart Structures and Systems*, 14(6):1221–1245, 2014.
15. M. Nakashima and N. Masaoka. Real-time on-line Test for MDOF Systems. *Earthquake Engineering & Structural Dynamics*, 28(4):393–420, April 1999.
16. M. Nakashima and N. Masaoka. Real-time on-line test for MDOF systems. *Earthquake Engineering & Structural Dynamics*, 28(4):393–420, April 1999.
17. Y. Ohtori, R. E. Christenson, B. F. Spencer, and S. J. Dyke. Benchmark Control Problems for Seismically Excited Nonlinear Buildings. *Journal of Engineering Mechanics*, 130:366–385, 2004.
18. M. I. Wallace, D. J. Wagg, and S. A. Neild. An adaptive polynomial based forward prediction algorithm for multi-actuator real-time dynamic substructuring. *Proceedings of the Royal Society A: Mathematical, Physical and Engineering Sciences*, 461:3807–3826, 2005.
19. Q. Wang and G. Parmer. Practical, predictable, and efficient system support for fork/join parallelism. *the 20th Real-Time and Embedded Technology and Applications Symposium (RTAS)*, 2014.